J. Fluid Mech. (1979), *vol.* 93, *part* 3, *pp.* 433–448
Printed in Great Britain

Large amplitude progressive interfacial waves

By JUDITH Y. HOLYER
Department of Applied Mathematics and Theoretical Physics, University of Cambridge†

(Received 1 May 1978 and in revised form 25 January 1979)

This paper contains a study of large amplitude, progressive interfacial waves moving between two infinite fluids of different densities. The highest wave has been calculated using the criterion that it has zero horizontal fluid velocity at the interface in a frame moving at the phase speed of the waves. For free surface waves this criterion is identical to the criterion due to Stokes, namely that there is a stagnation point at the crest of each wave. It is found that as the density of the upper fluid increases relative to the density of the lower fluid the maximum height of the wave, for fixed wavelength, increases. The maximum height of a Boussinesq wave, which has the density almost the same above and below the interface, is 2·5 times the maximum height of a surface wave of the same wavelength. A wave with air over the top of it can be about 2% higher than the highest free surface wave. The point at which the limiting criterion is first satisfied moves from the crest for free surface waves to the point half-way between the crest and the trough for Boussinesq waves. The phase speed, momentum, energy and other wave properties are calculated for waves up to the highest using Padé approximants. For free surface waves and waves with air above the interface the maximum value of these properties occurs for waves which are lower than the highest. For Boussinesq waves and waves with the density of the upper fluid one-tenth of the density of the lower fluid these properties each increase monotonically with the wave height.

1. Introduction

Over the past decades a large amount of work has been done on steady, progressive, free surface waves. Stokes (1880) asserted that the highest surface wave would have a stagnation point at the crest in a frame moving with the waves and from this he deduced that the wave must be sharp crested and enclose an angle of 120° at the crest. Stokes formulated the problem as a perturbation expansion and obtained the solution to third order for waves on an infinitely deep fluid. Levi-Civita (1925) proved Stokes' expansion was convergent for sufficiently small waves. The coefficients of the expansion have been calculated to higher orders by various authors and most recently by Schwartz (1974) and Cokelet (1977), who used digital computers to calculate the expansion to approximately 100th order. Using Padé approximants to sum these series, they determined the highest wave for various values of the water depth. Cokelet also calculated the mass, momentum and energy and their respective fluxes and showed that these and the phase speed achieved their maximum values for waves lower than the highest.

However, waves which occur in nature are never, in fact, free surface waves, since they are always beneath a fluid of some finite density, if only air. Despite this fact,

† Present address: Topexpress Ltd., 1 Portugal Place, Cambridge.

0022-1120/79/4280-7110 $02.00

very little work has been done on finite amplitude interfacial and internal waves. Benjamin (1966) considered finite amplitude effects on solitary and cnoidal waves in a stratified fluid. Hunt (1961) considered interfacial waves in a similar manner to that of Levi-Civita (1925) for surface waves and claimed to prove the convergence of the perturbation expansion for interfacial waves. Unfortunately this paper is incorrect, since the boundary conditions are incorrectly applied, and there is, at present, no proof of the convergence of the series expansion for interfacial waves. Tsuji & Nagata (1973) have correctly carried the expansion for interfacial waves to fifth order, which has provided a check on the present calculations.

None of the papers mentioned above has considered what limits the height of interfacial waves. The highest interfacial wave cannot have a stagnation point at the crest, since this would imply infinite velocity around the crest in the upper fluid. This criterion can only be true for free surface waves. A criterion that will limit the height of interfacial and internal waves will be that the horizontal fluid speed at some point in the fluid equals the phase speed. For interfacial waves this criterion is exactly equivalent to stating that the interface will become vertical at some point. If this point were the crest, as it is for free surface waves, there would be a stagnation point, since the vertical velocity is zero at the crest. The criterion is discussed further in § 4. Since the waves studied in this paper move along a sharp interface which has no surface tension, the waves will always be unstable to short wavelength perturbations. However, in any given physical situation there will always be either surface tension or a diffuse interface to stabilize short waves, and, provided that the shear across the interface is small enough, the waves will be first limited in height by the criterion that the interface becomes vertical. Orlanski & Bryan (1969) discuss this limiting criterion with reference to the thermocline in the ocean and give evidence to suggest that breaking by this mechanism occurs before the system becomes Kelvin–Helmholtz unstable. Thorpe (1978) also considers this criterion and in laboratory experiments, which include the effects of shear and a continuous stratification, he observes this type of wave breaking occurring before Kelvin–Helmholtz instability.

This paper considers large amplitude interfacial waves moving between two infinite fluids of different densities, which are at rest far from the interface. Using Padé approximants to sum the series, we calculate the height of the highest wave, applying the criterion that the highest wave will have the horizontal fluid speed equal to the phase speed at some point in the fluid. For surface waves this first occurs at the crest and the criterion becomes the same as that used by Stokes, namely that there is a stagnation point at the crest in the frame moving with the waves. For waves with non-zero density in the upper plane the waves can no longer be limited in height by the crest, since this would imply infinite velocity around the crest. Instead the interface first becomes vertical a short way from the crest. We show that Boussinesq waves, for which the density difference is only important when incorporated with gravity, attain the limiting criterion at their mid-height. This is because as Boussinesq waves get higher, for fixed wavelength, they flatten at the troughs and crests and the highest value of the surface slope is always at the mid-height, making this the point where the profile first becomes vertical, and thus the point where the horizontal fluid speed first equals the phase speed.

In § 5 we calculate the phase speed, wave momentum, kinetic and potential energies, the momentum flux and the energy flux of the waves. For free surface waves each of these properties reaches a maximum value for a wave amplitude less than the highest (Cokelet 1977). We confirm this result and show that it also happens if a fluid of about the density of air is over the waves. Thus it is possible to apply any consequences of this effect, such as those suggested by Longuet-Higgins & Fenton (1974), to the ocean or laboratory where, one assumes, there will always be air above the waves. For Boussinesq waves each of the wave properties increases monotonically with the wave height. We also consider an intermediate case in which the upper density is one tenth of the lower density and in this case the wave properties also increase monotonically with the wave height. The reason that only waves with a low density fluid on top can achieve a maximum in their properties is that it is only for these waves that the highest wave profile intersects that of slightly lower waves very near the crest, which makes the highest wave actually lower for most of the profile. For Boussinesq waves the profiles always intersect at the mid-height and the height of the wave at each point increases monotonically with the wave height, which makes a maximum impossible.

We also show that as the density of the upper fluid increases relative to the density of the lower fluid the maximum wave amplitude of the wave increases. The maximum amplitude of a Boussinesq wave is over twice the amplitude of a surface wave of the same wavelength. A wave with air over the top of it can be about 2 % higher than the highest free surface wave of the same wavelength.

2. Formulation of problem

We consider symmetrical, two-dimensional, periodic waves of wavelength λ and wavenumber $k = 2\pi/\lambda$ moving from left to right without change of form along an interface under the influence of gravity. Units of length and time are chosen so that $k = 1$ and $c_0^2 = g(\rho_1 - \rho_2)/(\rho_1 + \rho_2)k = 1$, where ρ_1 and ρ_2 are the densities of the fluids below and above the interface respectively, with $\rho_1 > \rho_2$. The phase speed of infinitesimal waves is c_0. The unit of length has been chosen so that the wavelength is always fixed at 2π. The fluids above and below the interface are assumed to be inviscid and incompressible and the motion irrotational. The reference frame is chosen so that the fluid velocity tends to zero as the distance from the interface tends to infinity. This defines the propagation speed c of the waves uniquely with respect to that frame.

We choose rectangular co-ordinates (x, y) with the x axis horizontal and the y axis vertically upwards. The interface is at $y = \eta$ and the origin is chosen so that the mean height of the interface $\bar{\eta}$ is zero and so that at $t = 0$, $x = 0$ is at the crest of a wave. Since the fluids are incompressible and irrotational, we can define stream functions, ψ_1 and ψ_2, and velocity potentials, ϕ_1 and ϕ_2, for the lower and upper fluids respectively, which satisfy Laplace's equation. These will be defined such that the velocity (u_1, v_1) in the lower fluid and (u_2, v_2) in the upper fluid may be written

$$u_1 = \frac{\partial \phi_1}{\partial x} = \frac{\partial \psi_1}{\partial y}, \quad u_2 = \frac{\partial \phi_2}{\partial x} = \frac{\partial \psi_2}{\partial y},$$

$$v_1 = \frac{\partial \phi_1}{\partial y} = -\frac{\partial \psi_1}{\partial x} \quad \text{and} \quad v_2 = \frac{\partial \phi_2}{\partial y} = -\frac{\partial \psi_2}{\partial x}.$$

If we were considering only surface waves ($\rho_2 = 0$) the next step would normally be to change to a frame of reference (X, Y) moving in the positive x direction with the waves, at speed c, in which the motion is time independent. There would then be a new velocity potential and stream function

$$\Phi_1 = \phi_1 - cx \quad \text{and} \quad \Psi_1 = \psi_1 - cy$$

and the problem would be solved to find $X(\Phi_1, \Psi_1)$ and $Y(\Phi_1, \Psi_1)$.

However, if $\rho_2 \neq 0$ we must consider the fluids both above and below the interface. For non-infinitesimal waves $\Phi_1 \neq \Phi_2$ at two points in contact on the interface, and Φ_1 and Φ_2 are Fourier series of each other. In order to apply boundary conditions on the interface $\Psi_1 = \Psi_2 = 0$ it is necessary to calculate Fourier series of Fourier series. The consequence of this is that there is now no gain, but a loss, from using the Φ, Ψ plane and so we continue the calculation in the x, y plane.

The boundary conditions will be pressure continuity at the interface and the kinematic conditions that the interface moves with the vertical velocity of the fluid.

We use Bernoulli's equation above and below the interface to obtain equations for the pressure,

$$\begin{aligned} p_1/\rho_1 &= -(\partial\phi_1/\partial t + \tfrac{1}{2}(\nabla\phi_1)^2 + gy) + K_1, \\ p_2/\rho_2 &= -(\partial\phi_2/\partial t + \tfrac{1}{2}(\nabla\phi_2)^2 + gy) + K_2, \end{aligned} \tag{2.1}$$

where K_1, K_2 are Bernoulli constants. We can combine these equations on $y = \eta$, where $p_1 = p_2$, to obtain

$$A_0 + \rho_1(\partial\phi_1/\partial t + \tfrac{1}{2}(\nabla\phi_1)^2 + g\eta) = \rho_2(\partial\phi_2/\partial t + \tfrac{1}{2}(\nabla\phi_2)^2 + g\eta) \quad \text{on} \quad y = \eta, \tag{2.2a}$$

where $A_0 = \rho_2 K_2 - \rho_1 K_1$.

The kinematic conditions can be written

$$\frac{\partial\eta}{\partial t} + \frac{\partial\phi_1}{\partial x}\frac{\partial\eta}{\partial x} = \frac{\partial\phi_1}{\partial y} \quad \text{on} \quad y = \eta, \tag{2.2b}$$

$$\frac{\partial\eta}{\partial t} + \frac{\partial\phi_2}{\partial x}\frac{\partial\eta}{\partial x} = \frac{\partial\phi_2}{\partial y} \quad \text{on} \quad y = \eta. \tag{2.2c}$$

We will be making no linearization but will solve the fully nonlinear problem above by a perturbation expansion. The boundary conditions are to be applied on $y = \eta$, but using Taylor's theorem we can expand them so they can be applied on $y = 0$. The conditions (2.2) then become:

$$\frac{\partial\eta}{\partial t} + \sum_{j=0}^{\infty} \frac{\partial\eta}{\partial x}\frac{\eta^j}{j!}\frac{\partial^{j+1}\phi_1}{\partial x\,\partial y^j} = \sum_{j=0}^{\infty}\frac{\eta^j}{j!}\frac{\partial^{j+1}\phi_1}{\partial y^{j+1}} \quad \text{on} \quad y = 0; \tag{2.3a}$$

$$\frac{\partial\eta}{\partial t} + \sum_{j=0}^{\infty} \frac{\partial\eta}{\partial x}\frac{\eta^j}{j!}\frac{\partial^{j+1}\phi_2}{\partial x\,\partial y^j} = \sum_{j=0}^{\infty}\frac{\eta^j}{j!}\frac{\partial^{j+1}\phi_2}{\partial y^{j+1}} \quad \text{on} \quad y = 0; \tag{2.3b}$$

$$\begin{aligned} &\rho_1\left(\sum_{j=0}^{\infty}\frac{\eta^j}{j!}\frac{\partial^{j+1}\phi_1}{\partial t\,\partial y^j} + \frac{1}{2}\sum_{j=0}^{\infty}\frac{\eta^j}{j!}\frac{\partial^j}{\partial y^j}(\nabla\phi_1)^2 + g\eta\right) + A_0 \\ &\qquad = \rho_2\left(\sum_{j=0}^{\infty}\frac{\eta^j}{j!}\frac{\partial^{j+1}\phi_2}{\partial t\,\partial y^j} + \frac{1}{2}\sum_{j=0}^{\infty}\frac{\eta^j}{j!}\frac{\partial^j}{\partial y^j}(\nabla\phi_2)^2 + g\eta\right) \quad \text{on} \quad y = 0. \end{aligned} \tag{2.3c}$$

Now we can expand η, ϕ_1, and ϕ_2 as Fourier series:

$$\eta = \sum_{n=1}^{\infty} a_n \cos n\theta; \tag{2.4a}$$

$$\phi_1 = \sum_{n=1}^{\infty} A_n e^{ny} \sin n\theta; \tag{2.4b}$$

$$\phi_2 = \sum_{n=1}^{\infty} B_n e^{-ny} \sin n\theta; \tag{2.4c}$$

where $\theta = x - ct$ and ϕ_1 and ϕ_2 have been chosen to satisfy Laplace's equation and the conditions that $\phi_1 \to 0$ as $y \to -\infty$ and $\phi_2 \to 0$ as $y \to +\infty$.

We write

$$(\partial/\partial y^j)((\nabla\phi_1)^2) = 2\sum_{n=0}^{\infty} Q_{n,j}\cos n\theta$$

and

$$(\partial/\partial y^j)((\nabla\phi_2)^2) = 2(-1)^j\sum_{n=0}^{\infty} R_{n,j}\cos n\theta, \tag{2.5}$$

where

$$Q_{n-1,j} = (n+1)^j A_1(nA_n)e^{(n+1)y} + (n+3)^j(2A_2)(n+1)A_{n+1}e^{(n+3)y} + \dots \quad (n > 1)$$

and

$$2Q_{0,j} = 2^j A_1^2 e^{2y} + 4^j(2A_2)^2 e^{4y} + \dots;$$

and

$$R_{n-1,j} = (n+1)^j B_1(nB_n)e^{-(n+1)y} + (n+3)^j(2B_2)(n+1)B_{n+1}e^{-(n+3)y} + \dots \quad (n > 1),$$

and

$$2R_{0,j} = 2^j B_1^2 e^{-2y} + 4^j(2B_2)^2 e^{-4y} + \dots .$$

We now substitute the expansions (2.4) and (2.5) into the boundary conditions (2.3) to obtain:

$$c\sum_{n=1}^{\infty} na_n \sin n\theta - \sum_{n=1}^{\infty} nA_n \sin n\theta = \sum_{j=0}^{\infty}\frac{\eta^j}{j!}\left(\sum_{m=1}^{\infty} m^{j+1}A_m\cos m\theta\right)\left(\sum_{n=1}^{\infty} na_n\sin n\theta\right) + \sum_{j=1}^{\infty}\frac{\eta^j}{j!}\left(\sum_{m=1}^{\infty} m^{j+1}A_m\sin m\theta\right); \tag{2.6a}$$

$$c\sum_{n=1}^{\infty} na_n \sin n\theta + \sum_{n=1}^{\infty} nB_n \sin n\theta = \sum_{j=0}^{\infty}\frac{(-\eta)^j}{j!}\left(\sum_{m=1}^{\infty} m^{j+1}B_m\cos m\theta\right)\left(\sum_{n=1}^{\infty} na_n\sin n\theta\right) - \sum_{j=1}^{\infty}\frac{(-\eta)^j}{j!}\left(\sum_{m=1}^{\infty} m^{j+1}B_m\sin m\theta\right); \tag{2.6b}$$

$$A_0 + (\rho_1-\rho_2)g\eta - \rho_1 c\sum_{n=1}^{\infty} nA_n\cos n\theta + \rho_2 c\sum_{n=1}^{\infty} nB_n\cos n\theta$$
$$= \sum_{j=0}^{\infty}\frac{\eta^j}{j!}\left(-\rho_1\sum_{n=0}^{\infty} Q_{n,j}\cos n\theta + (-1)^j\rho_2\sum_{n=0}^{\infty} R_{n,j}\cos n\theta\right)$$
$$+ \sum_{j=1}^{\infty}\frac{c\eta^j}{j!}\left(\rho_1\sum_{n=1}^{\infty} n^{j+1}A_n\cos n\theta + \rho_2\sum_{n=1}^{\infty}(-n)^{j+1}B_n\cos n\theta\right). \tag{2.6c}$$

We now assume expansions for a_n, A_n, B_n, A_0 and c of the form

$$\left.\begin{aligned} a_n &= \sum_{k=0}^{\infty} a_{n,2k}\epsilon^{n+2k}, \\ A_n &= c_0 \sum_{k=0}^{\infty} A_{n,2k}\epsilon^{n+2k}, \\ B_n &= c_0 \sum_{k=0}^{\infty} B_{n,2k}\epsilon^{n+2k}, \\ A_0 &= c_0^2 \sum_{k=0}^{\infty} A_{0,2k}\epsilon^{3+2k}, \\ c &= c_0 \sum_{k=0}^{\infty} c_{2k}\epsilon^{2k}. \end{aligned}\right\} \tag{2.7}$$

These expansions are similar to those made by Cokelet (1977) for surface waves. The expansion parameter, ϵ, must be specified in order to solve the problem. We choose here $\epsilon = a$, the semi-wave-height. This is the only possible reasonable choice for ϵ *a priori*, since, as yet, we do not know what the highest wave will be.

The semi-wave-height a is given by

$$a = \tfrac{1}{2}(\eta(0) - \eta(\pi)) = \sum_{n=1}^{\infty} a_{2n-1}.$$

Equating powers of ϵ in this equation we find

$$a_{1,0} = 1$$

and

$$a_{1,2n} = -\sum_{m=0}^{n-1} a_{2(n-m)+1,2k}. \tag{2.8}$$

Supposing that the right-hand sides of (2.6) can be written as, respectively,

$$\left.\begin{aligned} &c_0 \sum_{n=1}^{\infty} \sum_{m=0}^{[\frac{1}{2}n]} X_{n,m}\epsilon^n \sin m\theta, \\ &c_0 \sum_{n=1}^{\infty} \sum_{m=0}^{[\frac{1}{2}n]} Y_{n,m}\epsilon^n \sin m\theta, \\ \text{and}\quad &c_0^2 \sum_{n=1}^{\infty} \sum_{m=0}^{[\frac{1}{2}n]} Z_{n,m}\epsilon^n \cos m\theta, \end{aligned}\right\} \tag{2.9}$$

and equating coefficients of ϵ^n in (2.6), we get

$$\sum_{m=0}^{[\frac{1}{2}n]} \left(c_{2m} \left(\sum_{j=0}^{[\frac{1}{2}n]-m} (n-2m-2j)\, a_{n-2m-2j,2j} \sin(n-2m-2j)\,\theta \right) - (n-2m)\, A_{n-2m,2m} \sin(n-2_m)\,\theta \right) = \sum_{m=0}^{[\frac{1}{2}n]} X_{n,m} \sin m\theta, \tag{2.10a}$$

$$\sum_{m=0}^{[\frac{1}{2}n]} \left(c_{2m} \left(\sum_{j=0}^{[\frac{1}{2}n]-m} (n-2m-2j)\, a_{n-2m-2j,2j} \sin(n-2m-2j)\,\theta \right) + (n-2m)\, B_{n-2m,2m} \sin(n-2m)\,\theta \right) = \sum_{m=0}^{[\frac{1}{2}n]} Y_{n,m} \sin m\theta \tag{2.10b}$$

and

$$A_{0,n}+(\rho_1+\rho_2)\sum_{m=0}^{[\frac{1}{2}n]} a_{n-2m,\,2m}\cos(n-2m)\,\theta-\sum_{m=0}^{[\frac{1}{2}n]}\sum_{j=0}^{[\frac{1}{2}n]-m} c_{2m}$$
$$\times(n-2m-2j)\cos(n-2m-2j)\,\theta(\rho_1 A_{n-2m-2j,\,2j}-\rho_2 B_{n-2m-2j,\,2j}) = \sum_{m=0}^{[\frac{1}{2}n]} Z_{n,m}\cos m\theta, \tag{2.10c}$$

where $[\frac{1}{2}n]$ is the greatest integer not exceeding $\frac{1}{2}n$.

We can solve equations (2.10) using equation (2.8). First we equate coefficients of $\sin k\theta$ in (2.10*a*) and (2.10*b*) and coefficients of $\cos k\theta$ in (2.10*c*). The part of (2.10*c*) independent of θ gives

$$A_{0,n} = Z_{n,0}.$$

If n is even, only even k occurs in (2.10) and, if n is odd, only odd k occurs. When n and k are even, we obtain, for $k \geqslant 2$,

$$\left.\begin{aligned}
a_{k,n-k}-A_{k,n-k} &= \frac{X_{n,k}}{k}-\sum_{m=1}^{[\frac{1}{2}(n-k)]} c_{2m}a_{k,\,n-2m-k},\\
a_{k,n-k}+B_{k,n-k} &= \frac{Y_{n,k}}{k}-\sum_{m=1}^{[\frac{1}{2}(n-k)]} c_{2m}a_{k,\,n-2m-k},\\
-(\rho_1+\rho_2)(k-1)\,a_{k,n-k} &= Z_{n,k}-\rho_1 X_{n,k}-\rho_2 Y_{n,k}\\
&\quad+\sum_{m=1}^{[\frac{1}{2}(n-k)]} kc_{2m}(\rho_1 A_{k,\,n-2m-k}-\rho_2 B_{k,\,n-2m-k}+(\rho_1+\rho_2)\,a_{k,\,n-2m-k}).
\end{aligned}\right\} \tag{2.11}$$

When n and k are odd, provided $k \geqslant 3$, we can use (2.11). If $k = 1$ we do not know $a_{1,n-1}$, $A_{1,n-1}$, $B_{1,n-1}$ or c_{n-1}, so we use our fourth equation, (2.8), from which we find

$$a_{1,n-1} = -\sum_{k=1}^{[\frac{1}{2}(n-1)]} a_{1+2k,\,n-2k-1}.$$

Then the other equations become

$$\left.\begin{aligned}
c_{n-1}-A_{1,n-1} &= X_{n,1}-\sum_{m=0}^{[\frac{1}{2}(n-3)]} c_{2m}a_{1,\,n-1-2m},\\
c_{n-1}+B_{1,n-1} &= Y_{n,1}-\sum_{m=0}^{[\frac{1}{2}(n-3)]} c_{2m}a_{1,\,n-1-2m},\\
-2(\rho_1+\rho_2)\,c_{n-1} &= Z_{n,1}-\rho_1 X_{n,1}-\rho_2 Y_{n,1}\\
&\quad+\sum_{m=1}^{[\frac{1}{2}(n-3)]} c_{2m}(\rho_1 A_{1,\,n-1-2m}-\rho_2 B_{1,\,n-1-2m}+(\rho_1+\rho_2)\,a_{1,\,n-1-2m}).
\end{aligned}\right\} \tag{2.12}$$

3. Method of solution

The algebraic manipulations required to solve equations (2.11), (2.12) and (2.8) were programmed in FORTRAN IV on Cambridge University's IBM 370/165 computer, for different values of the densities ρ_1 and ρ_2. The coefficients at order ϵ^n were determined from the previously determined coefficients of lower order. At each even order, $2p$, the coefficients $X_{2p,\,2k}$, $Y_{2p,\,2k}$ and $Z_{2p,\,2k}$ were calculated for $k = 0, 1, \ldots, p$. Then $A_{0,\,2k}$ was found and $a_{2p-2k,\,2k}$, $A_{2p-2k,\,2k}$ and $B_{2p-2k,\,2k}$ were determined for

$$k = 0, 1, \ldots, (p-1).$$

At each odd order, $2p+1$, $X_{2p+1,\,2k+1}$, $Y_{2p+1,\,2k+1}$ and $Z_{2p+1,\,2k+1}$ were calculated for $k = 0, 1, \ldots, p$. Then $a_{2(p-k)+1,\,2k}$, $A_{2(p-k)+1,\,2k}$ and $B_{2(p-k)+1,\,2k}$ were found for

$$k = 0, 1, \ldots, (p-1).$$

Then $a_{1,\,2p}$ was found using (2.8), and so c_{2p}, $A_{1,\,2p}$ and $B_{1,\,2p}$ could be found.

The order to which the calculation has been taken was limited by the CPU time required, which is proportional to N^5. The execution time for a double precision calculation to order ϵ^{31} was about 15 minutes, independent of the densities chosen. Most of the time was taken in calculating the coefficients $X_{n,m}$, $Y_{n,m}$ and $Z_{n,m}$, for which many Fourier series must be multiplied together. It would be possible to make the time needed proportional to $N^4 \log N$ by using fast Fourier transforms to multiply these series. However, this algorithm would not actually become faster until $N \sim 32$, so it was not used. The surface wave calculations of Schwartz (1974) and Cokelet (1977) took time proportional to N^4 because it was only necessary for them to multiply two Fourier series which could be done explicitly and the ϵ^n coefficients could be extracted before programming the calculation.

The number of coefficients which has been obtained seems, however, to be sufficient for all the purposes required here, although higher accuracy would be obtained with more terms. There is no proof that the series for interfacial waves converge. Hunt (1961) claimed to prove the series converged for small values of the expansion parameter. However, he essentially assumed the velocity potential was continuous across the interface, which it is not, thus invalidating the proof. The series obtained here do seem to be convergent when taken as power series in the expansion parameter, at least for small wave heights. Even if the series is divergent the Padé approximants will give useful information. The Padé approximants always seem to converge for waves short of the highest.

Four different density configurations have been studied here.

(i) $\rho_2/\rho_1 = 0$. These are free surface waves which have been studied by others. They have been considered in order to make comparisons with previous work.

(ii) $\rho_2/\rho_1 = 0{\cdot}001$. These are waves with a fluid of approximately the density of air above them. These are useful in studying the effect of the air on surface waves. We shall call them air–water waves.

(iii) $\rho_2/\rho_1 = 0{\cdot}1$. These are waves of intermediate density used to examine the effect of changing the densities.

(iv) $\rho_2/\rho_1 = 1-\delta$, $\delta \to 0$. These are Boussinesq waves in which the density difference $(\rho_1-\rho_2)$ is only important when incorporated with gravity.

The accuracy of the program to calculate the series was checked in several ways. Schwartz (1974) gives the first six terms for the phase speed for surface waves as a series in our expansion parameter, a. These numbers were found to agree with those of the present calculation to about 15 decimal places, that is full machine accuracy. Unfortunately it is not possible to make a direct comparison with any of the other terms in the series owing to the different way in which he formulated the problem, but further comparisons were made later with surface waves and the agreement was good. Tsuji & Nagata (1973) calculated the series for interfacial waves to fifth order using the same expansion procedure but a different expansion parameter, namely $a_{1,\,0}$. By calculating the series for a in terms of $a_{1,\,0}$ it was possible to make a check on the accuracy to fifth order for any density configuration. Again this calculation agreed with theirs to full machine accuracy. We have calculated the series here to 31st order in the expansion parameter for each of the different densities and this gives sufficient accuracy to consider waves up to the highest.

4. Highest waves and surface profiles

Interfacial waves reach their maximum height when the horizontal fluid speed at some point in the fluid equals the phase speed. Because $\nabla^2(\partial\phi/\partial x) = 0$ in the interior of each fluid, $\partial\phi/\partial x$ will attain its extreme values on the interface, and so the horizontal fluid speed will first equal the phase speed on the interface. The height of the waves is limited by this condition. Consider the steady motion in a frame of reference moving forward at the phase speed of the waves. The particles by the interface are in general moving in the $-x$ direction. If the fluid speed exceeds the phase speed at some point in the flow the particle motion is reversed and the particle path, and hence the interface, must assume an S-shape through this point. Thus there is a region in which heavy fluid is above light fluid. For waves which are lower than the highest wave the horizontal fluid speed is always less than the phase speed. The difference between the horizontal speed and the phase speed decreases as the wave height increases.

In the frame which we are using this criterion can be written as $\partial\phi_1/\partial x - c = 0$. At the point where this occurs the interface will be vertical and so we must also have $\partial\phi_2/\partial x - c = 0$ at the same point. For surface waves this first occurs at the crest of the wave, giving a highest wave which has a stagnation point at the crest in the frame moving with the waves. For interfacial waves this cannot first occur at the crest, since to have a stagnation point at the crest of a wave would imply infinite velocity over the crest in the upper fluid. In order to determine the point along the interface at which breaking first occurs and to find the height of such a highest wave the value of $\partial\phi_1/\partial x - c$ is calculated using Padé approximants at points along the interface for different values of the semi-wave-height a.

We use $[N, N]$ Padé approximants to sum the series for the horizontal velocity in order to analytically continue the sum of the series. Given a series known to order z^{2N}

$$f(z) = a_0 + a_1 z + a_2 z^2 + \ldots + a_{2N} z^{2N}, \tag{4.1}$$

its Padé approximant $[N, N]f(z)$ can be defined by

$$[N, N]f(z) = \frac{b_0 + b_1 z + \ldots + b_N z^N}{1 + c_1 z + \ldots + c_N z^N}. \tag{4.2}$$

The coefficients b_i and c_i are found by equating powers of z up to order z^{2N} in (4.1) and (4.2). The theory of Padé approximants is not completely understood but they have been used with great success in the past in the theory of water waves by Schwartz (1974), Longuet-Higgins & Fenton (1974) and Cokelet (1977). None of the theorems yet proved about Padé approximants will make their use rigorous in applications such as these. The best references to date on the subject are Baker (1965) and Graves-Morris (1973).

In figure 1(a) the horizontal fluid velocity, $\partial\phi_1/\partial x - c$, at the crest of the surface wave is plotted as a function of a. The highest wave will have a wave height corresponding to the value for which $\partial\phi_1/\partial x - c$ equals zero. Based on the convergence on the Padé approximants the series becomes zero when the semi-wave-height a equals

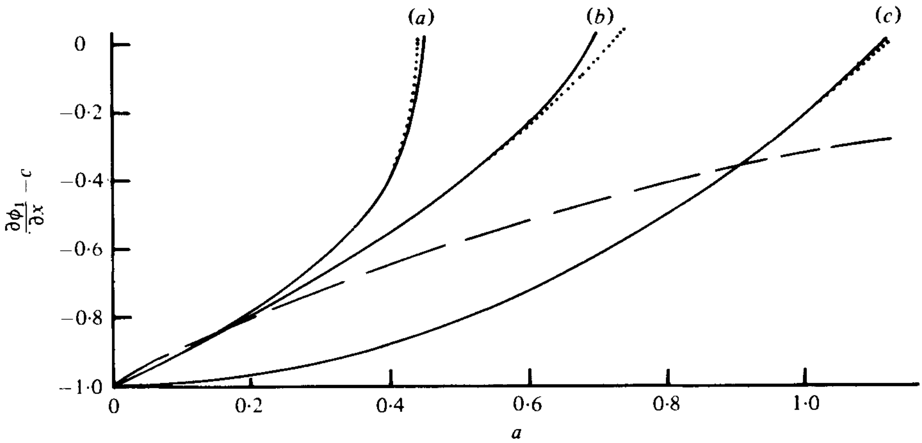

FIGURE 1. (a) The horizontal fluid velocity, $(\partial\phi_1/\partial x) - c$, at the crest of a surface wave. (b) The velocity at $\theta = \frac{1}{10}\pi$ with $\rho_2/\rho_1 = 0{\cdot}1$. (c) The velocity for Boussinesq waves. The solid line is the velocity at $\theta = \frac{1}{2}\pi$. The broken line is the velocity just below the crest, $\theta = 0$. For each figure the solid line is the [7, 7] approximant and the dotted line is the [6, 6] approximant. Where the dashed line is not present the two Padé approximants are too close for their difference to be visible.

$0{\cdot}445 \pm 0{\cdot}004$. This is a ratio of wave height to wavelength of $0{\cdot}1415 \pm 0{\cdot}001$. The value of this highest wave given by Cokelet is 0·141055. The value given by Cokelet is undoubtedly more accurate than that given here since we are using only 31 terms of our series, whereas he calculated 110 terms. Nevertheless this shows agreement within the accuracy of the present calculation.

For air–water waves the fluid velocity cannot first be zero at the crest. However, the point where the velocity does first become zero is so close to the crest that it cannot be found using only the number of terms in the series at present available. It is between $\theta = 0$ and $\theta = \pi/50$ with a maximum value of a of $0{\cdot}455 \pm 0{\cdot}004$; since at $\theta = 0$ and $a = 0{\cdot}451$ all the Padé approximants above [3, 3] are negative and at $a = 0{\cdot}459$ they are all positive, while at $\theta = \pi/50$ and $a = 0{\cdot}451$ all the approximants above [3, 3] are negative and at $a = 0{\cdot}459$ they are still negative. The highest air–water wave has a ratio of wave height to wavelength of $0{\cdot}1448 \pm 0{\cdot}001$. Thus the maximum wave height has increased due to the fluid on top of the wave by about 2 %.

For the case where $\rho_2/\rho_1 = 0{\cdot}1$ the horizontal fluid velocity first becomes zero at $\theta = \pi/10 \pm \pi/100$. The maximum semi-wave-height a increases to $0{\cdot}71 \pm 0{\cdot}02$ and the velocity at $\theta = \pi/10$ is shown in figure 1 (b). The ratio of wave height to wavelength is $0{\cdot}226 \pm 0{\cdot}006$.

For Boussinesq waves the wave first starts to break at the mid-height where $\eta = 0$ and $\theta = \frac{1}{2}\pi$. The maximum value of a is $1{\cdot}10 \pm 0{\cdot}02$ corresponding to a ratio of wave height to wavelength of $0{\cdot}35 \pm 0{\cdot}006$. In figure 1 (c) the solid line shows the horizontal fluid velocity at the mid-height. The dashed line on the same graph shows the value of the same function just below the crest. We see that the horizontal fluid velocity is always negative at the crest and is still negative when the velocity at the mid-height becomes zero.

We show in table 1 the heights of the highest waves and the position where they break for each of the different densities we have considered here.

ρ_2/ρ_1	a/π	Distance from crest where breaking first occurs
0	$0{\cdot}1415 \pm 0{\cdot}001$	0
0·001	$0{\cdot}1448 \pm 0{\cdot}001$	$\frac{1}{100}\pi \pm \frac{1}{100}\pi$
0·1	$0{\cdot}226 \pm 0{\cdot}006$	$\frac{1}{10}\pi \pm \frac{1}{100}\pi$
1·0	$0{\cdot}350 \pm 0{\cdot}006$	$\frac{1}{2}\pi$

TABLE 1

In figures 2(*a*)–(*c*) the interface profiles of the waves are shown for different values of the wave height below the highest for each of the waves considered. Their profiles have been calculated using the series for the profile

$$\eta = \sum_{n=1}^{\infty} a_n \cos n\theta, \quad a_n = \sum_{k=0}^{\infty} a_{n,2k}\epsilon^{n+2k}. \tag{4.3}$$

First the coefficients a_n were found by Padé approximating their series. Then the series for η is Padé approximated as a series in θ, for the series for η can be written as a power series

$$2\eta = \sum_{n=1}^{\infty} a_n e^{in\theta} + \sum_{n=1}^{\infty} a_n e^{-in\theta}. \tag{4.4}$$

This method is similar to that used by Schwartz and Cokelet to calculate the surface, although the representation of the surface here is somewhat simpler. For each a_n, if we have taken the expansion to order N, then we will know $[\frac{1}{2}(N-n)+1]$ terms in the series for a_n. Thus for large n there will not be many terms in the series and the Padé approximants will not be able to converge. We do not want to retain coefficients in the expansion which have not converged and in order to do this we calculate

$$E = \frac{[L,L]\,a_n - [L-1,L-1]\,a_n}{na}$$

for $n = 1, \ldots, N$. We take $L = 1, 2, \ldots$ until either $E < 0{\cdot}5 \times 10^{-3}$ or $L = [\frac{1}{4}(N-n)]$. If $E < 0{\cdot}5 \times 10^{-3}$, then we take $[L,L]\,a_n$ as the nth Fourier coefficient. If $L = [\frac{1}{4}(N-n)]$ then we take a_{n-1} as the largest usable Fourier coefficient. We have chosen $E < 0{\cdot}5 \times 10^{-3}$ rather than Cokelet's criterion of $E < 10^{-5}$, as this enables waves closer to the highest to be plotted.

5. Integral properties of waves

We calculate here the phase speed, wave momentum, kinetic and potential energies, the momentum flux and the energy flux of the waves. It is possible to extend the results of Longuet-Higgins (1975), who calculated relationships between these quantities for surface waves, to interfacial waves. We have already chosen axes so that the mean elevation

$$\bar{\eta} = \frac{1}{\lambda}\int_0^{\lambda} \eta\, dx \tag{5.1}$$

is zero. Similarly, by choice of reference frame, the circulation per unit length

$$C = \frac{1}{\lambda}\int_0^{\lambda} u\, dx \tag{5.2}$$

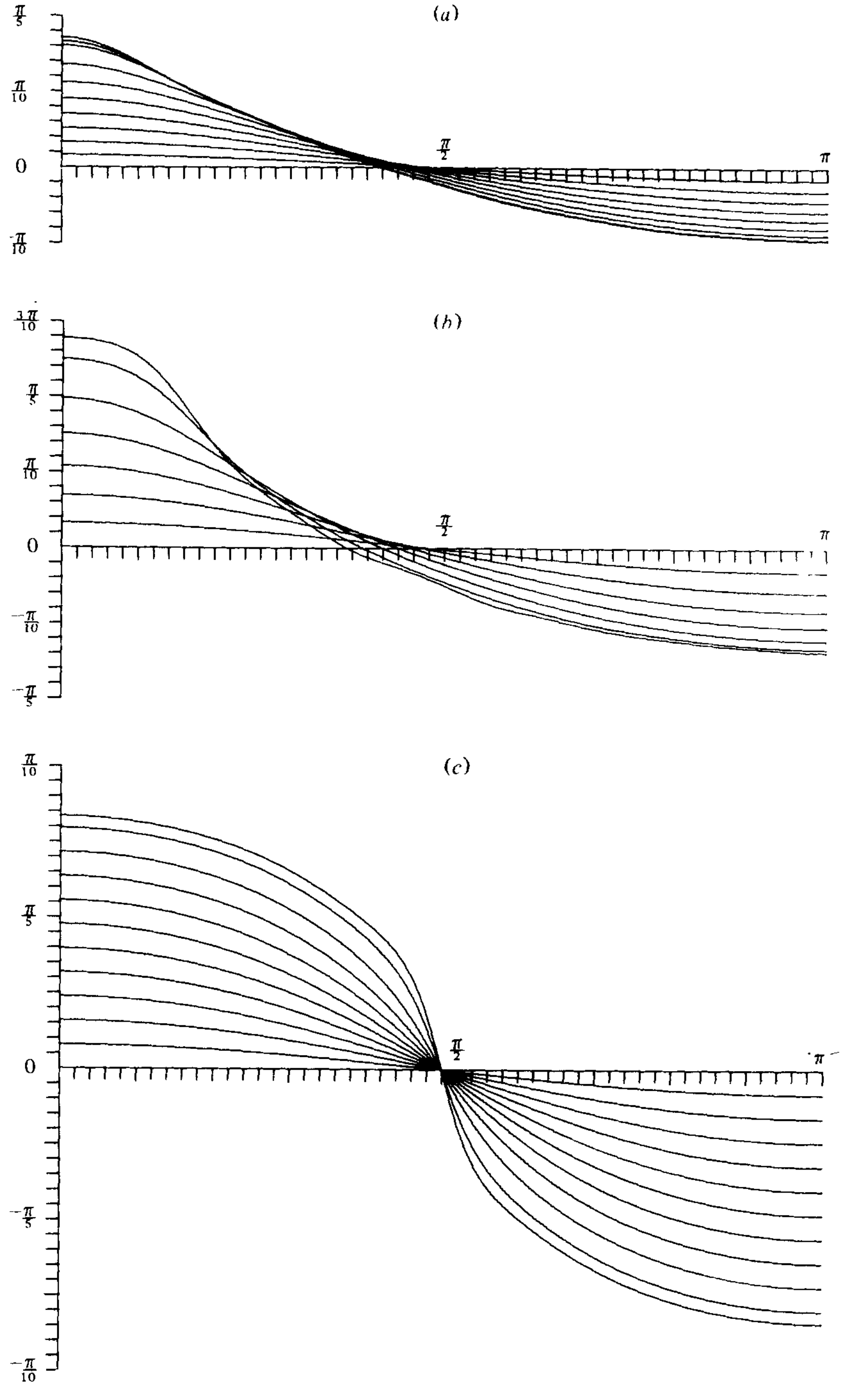

FIGURE 2. The surface profiles. (*a*) Surface waves at $a = 0{\cdot}05, 0{\cdot}1, \ldots, 0{\cdot}4, 0{\cdot}41, 0{\cdot}42$. (*b*) Waves with $\rho_2/\rho_1 = 0{\cdot}1$ at $a = 0{\cdot}1, 0{\cdot}2, \ldots, 0{\cdot}6, 0{\cdot}65$. (*c*) Boussinesq waves with $a = 0{\cdot}1, 0{\cdot}2, \ldots, 1{\cdot}0, 1{\cdot}05$.

is zero. We define the mean wave momentum or impulse per unit horizontal distance

$$I = \rho_1 \overline{\int_{-\infty}^{\eta} u\,dy} + \rho_2 \overline{\int_{\eta}^{\infty} u\,dy}, \tag{5.3}$$

the mean kinetic energy

$$T = \overline{\int_{-\infty}^{\eta} \tfrac{1}{2}\rho_1(u^2+v^2)\,dy} + \overline{\int_{\eta}^{\infty} \tfrac{1}{2}\rho_2(u^2+v^2)\,dy}, \tag{5.4}$$

the mean potential energy

$$\begin{aligned} V &= \overline{\int_{0}^{\eta} (\rho_1-\rho_2)\,gy\,dy} = \tfrac{1}{2}(\rho_1-\rho_2)\,g\overline{\eta^2} \\ &= \tfrac{1}{2}c_0^2(\rho_1+\rho_2)\,\overline{\eta^2}. \end{aligned} \tag{5.5}$$

The radiation stress, the excess flux of momentum due to the waves per unit span,

$$S_{xx} = \overline{\int_{-\infty}^{\eta} (p+\rho_1 u^2)\,dy} - \overline{\int_{-\infty}^{0} p_0\,dy} + \overline{\int_{\eta}^{\infty} (p+\rho_2 u^2)\,dy} - \overline{\int_{0}^{\infty} p_0\,dy}, \tag{5.6}$$

where p is the pressure and p_0 is the pressure in the absence of the waves. The mean energy flux

$$F = \overline{\int_{-\infty}^{\eta} (p+\tfrac{1}{2}\rho_1(u^2+v^2)+\rho_1 gy)\,u\,dy} + \overline{\int_{\eta}^{\infty} (p+\tfrac{1}{2}\rho_2(u^2+v^2)+\rho_2 gy)\,u\,dy}. \tag{5.7}$$

Longuet-Higgins (1975) has derived relationships between these quantities when $\rho_2 = 0$. These results are easily extended to interfacial waves when $\rho_2 \neq 0$. We omit the proofs here since they follow those of Longuet-Higgins very closely. The relationships are

$$\left.\begin{aligned} T &= \tfrac{1}{2}cI, \\ S_{xx} &= 4T-3V, \\ \text{and}\qquad F &= c(3T-2V). \end{aligned}\right\} \tag{5.8}$$

I and V were calculated by substituting in the series for u and η [(2.4) and (2.7)], obtaining the series

$$\left.\begin{aligned} I &= c_0 \sum_{n=1}^{\infty} I_n \epsilon^{2n} \\ \text{and}\qquad V &= c_0^2 \sum_{n=1}^{\infty} V_n \epsilon^{2n}. \end{aligned}\right\} \tag{5.9}$$

These, and the series for c [see (2.7)] ,were $[N, N]$ Padé approximated. The kinetic energy, momentum flux and energy flux were then calculated by means of the relations (5.8). The results are shown graphically in figures 3(a)–(d) and are available in tabular form from the author or the editorial office of the *Journal of Fluid Mechanics*.

For free surface waves we see there is a maximum in the phase speed c and each of the quantities I, T, V, S_{xx} and F for waves short of the highest. For air–water waves the quantities I, T, V, S_{xx} and F have maxima. The error in the phase speed c is too large to be certain whether or not there is a maximum, although the fact that the other wave properties do, suggests the phase speed also has a maximum. The Boussinesq waves and the waves with fluids of densities such that $\rho_2/\rho_1 = 0{\cdot}1$ do not

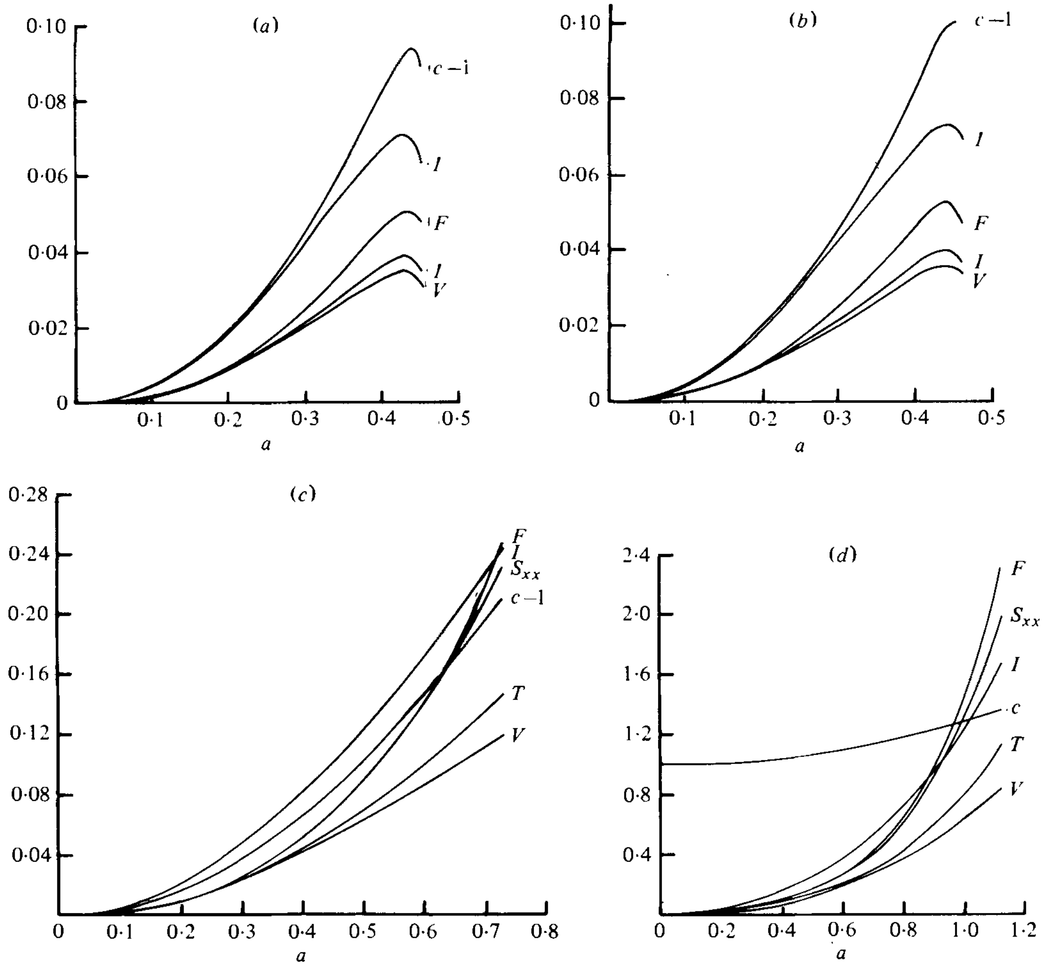

FIGURE 3. The wave properties c, I, T, V, S_{xx} and F for (*a*) surface waves, (*b*) air–water waves, (*c*) waves with $\rho_2/\rho_1 = 0{\cdot}1$, (*d*) Boussinesq waves. They are each plotted to the maximum value of a.

exhibit maxima in any of their properties, but increase monotonically with the wave height. These dimensionless versions of the wave properties increase as the upper density increases, thus the highest Boussinesq wave moves faster than any other wave relative to its infinitesimal wave speed.

6. Discussion

We have shown here the difference in limiting forms between surface waves and interfacial waves. The maximum height which interfacial waves of a given wavelength can attain, increases as the density ratio of the fluids increases. For surface waves the maximum value of wave height to wavelength ratio is about 0·14 and for Boussinesq waves the maximum value is about 0·35. The point at which the limiting criterion is first satisfied moves from the crest for surface waves to the mid-height for interfacial waves.

For waves on an almost free surface with a fluid of small, but finite, density above the wave, the waves can be slightly higher than free surface waves before breaking occurs. Moreover they are not limited by the velocity at the crest, but by the horizontal velocity at a point a short distance away. These waves still have a maximum in their wave properties making it possible to consider the consequences of the maximum in connexion with waves occurring naturally in the laboratory or on the oceans.

When the interfacial waves start to break there will be heavy fluid over light fluid and one may expect Rayleigh–Taylor instability and mixing. The flow may again become stable with rotors, regions of closed streamlines moving at the phase speed of the waves. There have not been many observations of finite amplitude interfacial or internal waves. Thorpe (1968*b*) obtains experimentally progressive finite amplitude interfacial waves in a fluid otherwise at rest, and compares with the third-order results for the interface shape. The waves he observes are not, however, nearly high enough to be breaking. Thorpe (1978) studies internal waves in a shear flow and shows experiments where breaking occurs before Kelvin–Helmholtz instability. The most familiar naturally occurring example of internal waves is in the ocean summer thermocline, where the situation is again complicated by shear. Woods (1968) has made observations of waves in the step-structure of the thermocline, but it appears that the waves he observed were breaking by Kelvin–Helmholtz instability, as the shear was sufficiently high and the waves themselves were not high enough to be breaking. Thorpe (1968*a*) has done experiments on standing waves between two fluids of similar densities and observed some sort of breaking taking place at the node. This could be a shear instability generated by the flow of the wave, as he suggests, but it seems possible that it is wave breaking.

I should like to thank Dr H. E. Huppert for his encouragement in this work and for his help in preparing this paper. I should also like to thank Dr S. A. Thorpe for bringing the paper by Tsuji and Nagata to my attention and Dr D. R. Moore for some advice on the computing. I am grateful to the Natural Environment Research Council for providing financial support.

REFERENCES

BAKER, G. A. 1965 The theory and application of the Padé approximant method. In *Advances in Theoretical Physics* (ed. K. Breuckner), vol. 1, p. 1. Academic Press.

BENJAMIN, T. B. 1966 Internal waves of finite amplitude and permanent form. *J. Fluid Mech.* **25**, 241.

COKELET, E. D. 1977 Steep gravity waves in water of arbitrary uniform depth. *Phil. Trans. Roy. Soc.* A **286**, 183.

GRAVES-MORRIS, P. R. 1973 *Padé Approximants and Their Applications*. London: Academic Press.

HUNT, J. N. 1961 Interfacial waves of finite amplitude. *La Houille Blanche* **16**, 515.

LEVI-CIVITA, T. 1925 Détermination rigoureuse des ondes permanentes d'ampleur finie. *Math. Ann.* **93**, 264.

LONGUET-HIGGINS, M. S. 1975 Integral properties of periodic gravity waves of finite amplitude. *Proc. Roy. Soc. Lond.* A **342**, 157.

LONGUET-HIGGINS, M. S. & FENTON, J. D. 1974 On the mass, momentum, energy and circulation of a solitary wave. II. *Proc. Roy. Soc.* A **350**, 1.

ORLANSKI, I. & BRYAN, K. 1969 Formation of the thermocline step structure by large amplitude internal gravity waves. *J. Geophys. Res.* **74**, 6975.

Schwartz, L. W. 1974 Computer extension and analytic continuation of Stokes' expansion for gravity waves. *J. Fluid Mech.* **62**, 553.

Stokes, G. G. 1880 Considerations relative to the greatest height of oscillatory irrotational waves. In *Mathematical and Physical Papers*, vol. 1, p. 225. Cambridge University Press.

Thorpe, S. A. 1968*a* On standing internal gravity waves of finite amplitude. *J. Fluid Mech.* **32**, 489.

Thorpe, S. A. 1968*b* On the shape of progressive internal waves. *Phil. Trans. Roy. Soc.* A **263**, 563.

Thorpe, S. A. 1978 On the shape and breaking of finite amplitude internal gravity waves in a shear flow. *J. Fluid Mech.* **85**, 7.

Tsuji, Y. & Nagata, Y. 1973 Stokes' expansion of internal deep water waves to the fifth order. *J. Ocean. Soc. Japan* **29**, 61.

Woods, J. D. 1968 Wave induced shear instability in the summer thermocline. *J. Fluid Mech.* **32**, 791.